emitted at 510 nm with activation at 340 nm to fluorescence emitted at 510 nm with activation at 380 nm. After calibration, the ratio values were transformed to absolute $[Ca^{2+}]_i$ values with the following equation: $R = R_{max} + (R_{min} - R_{max})/\{1 + ([Ca^{2+}]_i/K_d)^b\}$, where $R$ denotes F340/F380, $R_{max}$ and $R_{min}$ are the values of $R$ when the concentration of $Ca^{2+}$ is at a maximum and a minimum, respectively, and $K_d$ is the dissociation constant of fura 2-AM for $Ca^{2+}$ (240 nM). The value of $b$, which determines the degree of asymmetry, was 1.2. TEA was added by perfusion of 5 ml of a modified BSS solution containing 100 mM TEA and low NaCl (50 mM). Other components were not changed (see above for BSS composition). Bombsein was applied by addition of 1 ml of BSS plus 2 μM bombesin to a dish containing 1 ml of BSS (final bombesin concentration = 1 μM). Solution were applied within 0.5 cm of the cells whose responses were measured.

18. B. Sakmann and E. Neher, *Single-Channel Recordings* (Plenum, New York, 1983); A. S. French and L. L. Stockbridge, *Proc. R. Soc. London* **232**, 395 (1988).
19. J. A. Connor, *Cell Calcium* **14**, 185 (1983).
20. D. L. Alkon, *Sci. Am.* **260**, 42 (1989).
21. G. Tesco, M. Vergelli, L. Amaducci, S. Sorbi, *Exp. Gerontol.* **28**, 51 (1993).
22. L. A. Borden, F. R. Maxfield, J. E. Goldman, M. L. Shelanski, *Neurobiol. Aging* **13**, 33 (1991).

23. We thank Hamamatsu Photonics Corporation that generously provided the $Ca^{2+}$-imaging equipment used in this study. We also thank J. Schwartz for the use of the cell culture facility.

29 November 1993; accepted 10 February 1994

## TECHNICAL COMMENTS

# High-Pressure Melting of $(Mg,Fe)SiO_3$-Perovskite

We commend Zerr and Boehler on their high-pressure melting study of Mg-silicate perovskite (*1*). However, we disagree with their interpretation of earlier studies and their own experiments.

Contrary to what Zerr and Boehler state (*1*, p. 554), we have previously visually observed the melting of perovskite and other materials in situ at high pressures and temperatures (*2–8*), including forced convection across molten zones of about 5 to 30 μm in diameter, similar to that described by Zerr and Boehler. We also determined temperature variations across our samples, both experimentally and theoretically (*3, 9, 10*).

Zerr and Boehler state that the melting data of Jeanloz and co-workers (*4, 11*) "are in strong contradiction to" more recent measurements by Sweeney and Heinz (*12*). This suggests a lack of reproducibility among the earlier experiments. Yet, there is no contradiction, as Sweeney and Heinz explained that their "data do not represent the true melting temperature of iron-magnesium-silicate perovskite" (*13*). Instead, Sweeny and Heinz reported average field-of-view temperatures across their samples for which the correlation between laser power and measured temperature showed a break in slope (*12*). In general, it is not known how precisely the correlation of laser power and (average) temperature reproduces melting temperatures obtained using other criteria, but it is known that the average temperatures reported by Sweeney and Heinz must be far below the true melting temperature; hence, their cautionary note. Indeed, when a first-order correction is applied for the difference between average and peak temperatures within the sample, Sweeney and Heinz find relatively good agreement with the earlier studies (that is, within mutual uncertainties) over the pressure range examined by Zerr and Boehler.

A critical issue not addressed by Zerr and Boehler is the nature of the temperature gradients across their samples. That there must be gradients is well established, both empirically and theoretically, for *any* laser heating experiment in the diamond cell (*9, 10*). This is equally true for a Nd:YAG (*3, 6, 8, 9*) or a $CO_2$ (*14, 15*) heating laser because the intensity distribution across a laser beam is Gaussian, resulting in a spatially variable heat source within a sample (*16*). Also, diamonds represent nearly infinite and perfect heat sinks because of their dimensions (*17*) and because of the high thermal conductivity of diamond. Therefore, the nonuniformity of both heat sources and heat sinks must inevitably produce three-dimensional temperature gradients across the sample area (*9, 10*). In fact, it is the (time-fluctuating) spatial variations in temperature that induce the convection observed within the molten zone.

That large temperature gradients occur in the experiments of Zerr and Boehler (*1*), as there must physically be, is evident from their figure 2, which shows a molten zone (now quenched) about 30 μm in diameter, surrounded by about 15 μm of perovskite that is, in turn, rimmed by untransformed starting material (orthopyroxene). For such an experiment at 62.5 GPa, they report a melting temperature of 5000 (± 300) K. The high-pressure melting point is the temperature at the interface at which melt was in contact with crystalline perovskite, here located only 15 μm away from the untransformed starting material. Yet it is known that, at pressures above 20 to 25 GPa, pyroxene transforms to perovskite when heated to temperatures exceeding 1000 to 1300 K (*18*). Therefore, temperature differences of at least 3700 K (5000 K to 1300 K) must have existed over a radial distance of about 15 μm. The corresponding temperature gradient of about $10^8$ to $10^9$ K per meter is in good accord with our previous theoretical and experimental findings (*10, 19*).

Somewhat lower temperature gradients may be inferred if Zerr and Boehler were assuming that the temperature is constant across the convecting molten zone. For a Gaussian heat source, as is the case here, the resulting temperature distribution in the diamond cell is often found to be Gaussian, though with some notable exceptions (*6, 9, 10*). Assuming such a temperature distribution, we can fit Zerr and Boehler's temperature measurement at the center of their hot spot [note 5 in (*1*)], while constraining the temperature to be less than 1000 to 1300 K in the untransformed pyroxene. Doing so, we obtain a focal-spot diameter comparable to that of Zerr and Boehler [figure 1 in (*1*)] (*20*), and a temperature of 3100 (± 400) K at a radial distance of 15 μm from the hot-spot center, the location of the crystal-melt interface. This value is in good agreement with the melting temperatures reported by our groups and by others for silicate perovskite at 50 to 65 GPa (*4, 11, 12, 21*).

There could be many reasons for the differences between the Mainz results and other groups' measurements. Among other technicalities, sample configurations, optical components, methods of temperature determination, and criteria for constraining the high-pressure melting curve all differ in detail (*22*). Nevertheless, it is clear that temperature gradients must be quantified in the $CO_2$-laser heated diamond cell (*14, 15*). These gradients are sensitive to the configuration and properties of the sample and surrounding medium, configurations and properties that change as the sample is taken to successively higher pressures (for example, thinning of the sample under compression) (*9, 10*). A direct association of the peak temperature with a melting slope, without a characterization of the temperature distribution, is therefore unreliable.

**Dion L. Heinz**
*Department of Geophysical Sciences* and
*James Franck Institute,*
*University of Chicago,*
*Chicago, IL 60637, USA*
**Elise Knittle**
*Earth Sciences Board* and
*Institute of Tectonics,*
*University of California,*
*Santa Cruz, CA 95064, USA*
**Jeffrey S. Sweeney**
*Department of Geophysical Sciences*
*University of Chicago*
**Quentin Williams**
*Earth Sciences Board* and
*Institute of Tectonics,*
*University of California*

*Raymond Jeanloz*
*Department of Geology and Geophysics,*
*University of California,*
*Berkeley, CA 94720–4767, USA*

## REFERENCES AND NOTES

1. A. Zerr and R. Boehler, *Science* **262**, 553 (1993).
2. R. Jeanloz and D. L. Heinz, *J. Physique* (*Paris*) **45**, (C8) 83 (1984).
3. ———, in *Proceedings of the International Conference on Applications of Lasers and Electro-Optics*, C. Albright, Ed. (Springer-Verlag, New York, 1986), pp. 239–243.
4. D. L. Heinz and R. Jeanloz, *J. Geophys. Res.* **92**, 11437 (1987).
5. Q. Williams, R. Jeanloz, J. Bass, B. Svendsen, T. J. Ahrens, *Science* **236**, 181 (1987).
6. B. K. Godwal *et al.*, *ibid.* **248**, 462 (1990).
7. Q. Williams and R. Jeanloz, *J. Geophys. Res.* **95**, 19299 (1990).
8. Q. Williams *et al.*, *ibid.* **96**, 2171 (1991).
9. D. L. Heinz and R. Jeanloz, in *High-Pressure Research in Mineral Physics*, M. Manghnani and Y. Syono, Eds. (American Geophysical Union, Washington, DC, 1987), pp. 113–127.
10. S. Bodea and R. Jeanloz, *J. Appl. Phys.* **65**, 4688 (1989).
11. E. Knittle and R. Jeanloz, *Geophys. Res. Lett.* **16**, 421 (1989).
12. J. S. Sweeney and D. L. Heinz, *ibid.* **20**, 855 (1993). A highly stabilized laser-heating system was used in this study [D. L. Heinz, J. S. Sweeney, P. Miller, *Rev. Sci. Instr.* **62**, 1568 (1991)]. Although there are differences in detail (possibly associated with differing techniques and criteria used), this work confirmed the finding (*11*) that the melting behavior of silicate perovskite changes qualitatively at pressures above about 60 GPa.
13. See figure 2 in (*12*), for example.
14. R. Boehler and A. Chopelas, in *High-Pressure Research: Application to Earth and Planetary Sciences*, Y. Syono and M. H. Manghnani, Eds. (American Geophysical Union, Washington, DC, 1992), pp. 55–60.
15. T. Yagi and J. Susaki, *ibid.*, pp. 51–54.
16. Whether on the focal plane or off it, the power distribution across the beam is Gaussian for the $TEM_{00}$ mode that is commonly used (*9, 10, 14, 15*); higher modes also follow Gaussian intensity distributions, but modulated by Hermite polynomials [see for example, M. Young, *Optics and Lasers* (Springer-Verlag, New York, ed. 2, 1984).
17. The ratio of sample to diamond mass is less than $5 \times 10^{-6}$ in Zerr and Boehler's experiments (*1*), for example. The presence of the thin layer of pressure medium around the sample does not significantly influence our conclusion, regardless of the nature of the medium (for example, Ar).
18. E. Ito and E. Takahashi, *J. Geophys. Res.* **94**, 10637 (1989). Lower temperatures may suffice, but we do know that pyroxene does not transform on experimental time scales at 300 K.
19. Here, as elsewhere (*3–10*), we quote the maximum gradient in the temperature distribution. There has been some confusion when others have specified the minimum gradients in their experiments. Quoting the minimum value conveys no information because symmetry requires the temperature gradient to be zero at the exact center of the hot spot in the laser-heated diamond cell.
20. The characteristic radial dimension $\rho \sim 20$ to 25 μm, implying a beam "waist" of $2\rho \sim 40$ to 50 μm, which is in good accord with our own experimental and theoretical findings (our laser and optical components combine to yield $\rho \sim 10$ to 15 μm) (*9, 10*).
21. W. A. Bassett, M. S. Weathers, E. Huang, M. Onomichi, *Eos* **69**, 1451 (1988).
22. Calibrations have not been published (*1, 14*) to compare with multiple calibration experiments described in our earlier papers [for example (*2, 6, 9*); E. Knittle and R. Jeanloz, *J. Geophys. Res.* **96**, 16169 (1991)].

18 November 1993; accepted 22 December 1993

*Response*: We disagree with the comment by Heinz *et al.* on our work (*1*) because it does not account for the fundamental differences in the two laser-heating experiments. It does not address inadequacies in their experimental approaches to the measurement of melting at high pressure (*2, 3, 4, 5*) that have most likely led to large errors in estimates of the melting temperatures of two of the most important Earth materials, iron and (Mg,Fe)$SiO_3$-perovskite. Here, we briefly describe four significant improvements in laser-heating experiments and compare the different experimental approaches. These differences have been described in great detail by us elsewhere (*6, 7, 8*).

The two techniques used to heat silicate samples in the diamond cell can be compared (Fig. 1). In all three previous measurements (*2, 3, 4*) the sample acted as its own pressure medium (Fig. 1A, left side). The radiation of the Nd:YAG laser ($\lambda$ = 1.06 μm) was only weakly absorbed and thus had to be tightly focused. This created an extremely small hot spot, which due to the high thermal conduction of the sample (and even more, of the diamond anvils) was located somewhere in the center of the sample. It is physically impossible to measure the temperature in the center of such a hot spot because of large temperature gradients in the optical axis. In addition, the optical arrangement used earlier (*2, 3, 4*) only allowed the measurement of emitted light from a much larger volume surrounding the hot spot (Fig. 1B). Thus, the peak temperature of the hot spot could not be measured in these experiments, and had to be estimated. The calculation of the large (>1000 K/μm), three-dimensional, and asymmetric temperature gradients inevitably led to large uncertainties in such calculations.

The experiment that we developed over the last few years (*6, 7, 8*) is significantly different. In order to drastically reduce temperature gradients and thus large uncertainties, we used (i) thin (<15 μm) disks of samples, (ii) a pressure medium possessing low thermal conductivity (argon), and (iii) a $CO_2$ laser with a radiation ($\lambda$ = 10.6 μm) that is almost fully absorbed by silicates, and with a power that is greater than that of a YAG laser by about a factor of 8. This allowed defocused laser beams to heat the sample. Because of this cell geometry (Fig. 1A, right side) and heating technique, radial temperature gradients in the sample were significantly reduced, and the axial temperature gradients in the sample became negligible. The Ar surrounding the sample experienced extremely large temperature gradients, but did not emit light. Thus, previously three-dimensional temperature gradients in the sample were changed to a nearly two-dimensional distribution. Contrary to the assumption made by Heinz *et al.*, Ar is extremely effective as a thermal insulator as evident from the fact that drastic increases are required in laser power in cases where the sample contacted the diamond.

Temperatures were directly measured from small spots using pinhole apertures in the optical system. This method allowed for the precise measurement of peak temperatures and temperature gradient. We showed, that for the heating described above, temperature gradients within the sampled area were negligible (Fig. 2) (*6, 9*). We therefore disagree with the statement by Heinz *et al.* that we did not address this issue.

We further showed (*8*) that the measurement of temperatures from laser-heated spots requires the use of chromatically corrected collecting optics. Conventional lens systems used in all previous measurements (*2, 3, 4*) lead to large temperature uncertainties that occur when the size of the hot spot becomes small as compared with the chromatic aberration of the lens (for example, at higher pressures).

Although melting has been observed visually in previous measurements by convective motion, the temperatures at the solid-liquid transition (for example at the onset of melting) was never measured di-

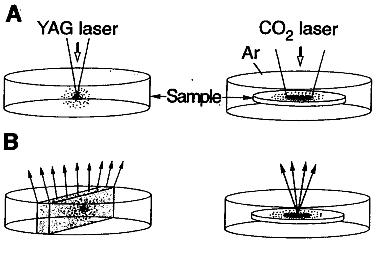

**Fig. 1.** Comparison of high-pressure cell assemblage, heating technique (**A**), and temperature measurement (**B**) in the laser heating experiments by Heinz *et al.* (*2–4*) (left side) and by Zerr and Boehler (*1*) (right side).

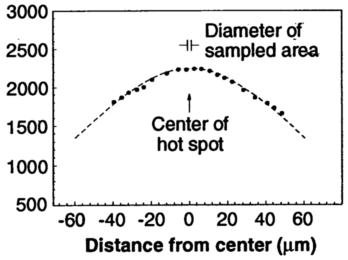

**Fig. 2.** Directly measured temperatures across a laser-heated mineral thin section embedded in Ar measured from 2-μm-diameter spots. (*9*). Temperature gradients within the sampled area in the center of the hot spot [3 to 5 μm in diameter (*1*)] are negligible. Data follow a Gaussian distribution.

rectly (*4*). In our experiment the peak temperature in the sample was directly measured while the laser power was slowly increased. As soon as melting occurred in the hottest portion of the sample, the absorption increased drastically, leading to "runaway" melting and subsequent melting phenomena [figure 2B of (*1*)]. The melting temperatures we reported are the last temperatures of the solid before melting set in. We stated (*1*, p. 554) that melting temperatures were recorded at the onset and not during melting. Temperatures measured during melting were very much higher and the emission spectra were of poor quality, which was most likely due to rapid temperature fluctuations caused by convection in the molten sample.

From figure 2B of our report, Heinz *et al.* inappropriately estimate temperature gradients in our sample based on the assumption that its outer portion did not convert to perovskite. No such statement was made in our report. We only stated that the sample surrounding the molten area was perovskite. More correctly: All of the sample surrounding the molten area had converted to perovskite. To avoid confusion, we would like to emphasize the statement in our report (*1*) that figure 2B represents conditions *after* a melting experiment, which are significantly different from those at the onset of melting.

Heinz *et al.* discount the drastic differences in their three previous estimates of melting. Curves showing zero, positive, or negative slopes, respectively, are clearly in disagreement with each other (*2*, *3*, *4*).

We fully agree with the statement of Heinz *et al.* that "A direct association of the peak temperature with a melting slope, without a characterization of the temperature distribution, is therefore unreliable."

**R. Boehler**
**A. Zerr**
*Max-Planck-Institut für Chemie,*
*Postfach 3060,*
*55020 Mainz, Germany*

## REFERENCES

1. A. Zerr and R. Boehler, *Science* **262**, 553 (1993).
2. D. L. Heinz and R. Jeanloz, *J. Geophys. Res.* **92**, 11437 (1987).
3. E. Knittle and R. Jeanloz, *Geophys. Res. Lett.* **16**, 421 (1989)
4. J. S. Sweeney and D. L. Heinz, *ibid.* **20**, 855 (1993)
5. Q. Williams, R. Jeanloz, J. Bass, B. Svendsen, T J. Ahrens, *Science* **236**, 181 (1987).
6. R. Boehler, N. von Bargen, A. Chopelas, *J. Geophys. Res.* **95**, 21731 (1990).
7. R. Boehler and A. Chopelas, *Geophys. Res. Lett.* **18**, 1147 (1991).
8. ______, in *High-Pressure Research: Application to Earth and Planetary Sciences*, Y. Syouo and M. H. Manghnani, Eds. (Terra Scientific, Tokyo, Japan, 1992), pp. 55–60.
9. R. Boehler, in *Metals Mater. Processes* **3**, 261 (1992).

15 December 1993; accepted 22 December 1993

---

# Statistical Analyses of Soil Quality

J. P. Reganold *et al.* (*1*) compare the properties of soil from biodynamic and conventional farms in the North Island of New Zealand and conclude that the biodynamic farms have "better soil quality." They collected soil samples from comparable parts of adjacent farms [table 2 in (*1*)], but the statistical inference tests performed with data from those samples led to "pseudoreplication" (*2*). Although Reganold *et al.* state that soil-forming factors were the same for each farm in each pair or set, it seems most unlikely that one could characterize these factors sufficiently to justify the use of such statistical methods.

The comparison by Reganold *et al.* of the aggregated data is especially problematic. A valid statistical comparison (that would avoid pseudoreplication) would treat each farm pair or set as a replicate block and analyse the data on that basis. This can be done by analyzing the data in table 2 of the report by Reganold *et al.* with a two-way analysis of variance (ANOVA) using a block design [(biodynamic as opposed to conventional farm) × block], with $n = 7$ blocks (*3*). Such an analysis [(Table 1), which is similar to table 3 of (*1*)] shows that the overall means of the soil properties are slightly different from those presented by Reganold *et al.* (*1*). Of greater concern is the fact that only one soil property (mineralizable N) of the 12 that were identified in table 3 of their report as differing significantly ($P < 0.01$) between conventional and biodynamic farms actually appears to be so.

The three biological indicators used by Reganold *et al.* do not seem to be appropriate for measuring the quality of soil life under biodynamic farming. (i) Greater soil respiration was assumed to be beneficial. But a loss of $CO_2$ from soils can indicate ecosystem inefficiency, that is, energy loss from the soil system. High ecosystem respiration (especially per unit biomass) often results from stress and disturbance factors (*4*). (ii) The ratio of mineralizable N to C is indicative of microbial N availability rather than microbial activity. (iii) Although earthworms are susceptible to some aspects of conventional farming (*5*), the data about earthworms presented by Reganold *et al.* (*1*, p. 347) are not replicated because samples were taken from only one biodynamic and one conventional farm.

Finally, the apparent advantages of biodynamics farming may be a result of prac-

**Table 1.** Comparison of soil properties from biodynamic and conventional farms. Mean value of aggregated soils data reanalyzed by Wardle with a 7 × 2 block design. Differences calculated by Reganold *et al.* and by Wardle. Abbreviations: bio, biodynamic; con, conventional; NS, not statistically significant; and S, statistically significant.

| Soil property | Mean value* |  | Difference† |  |
|---|---|---|---|---|
|  | All bio farms | All con farms | Indicated by Reganold *et al.*† | *P* calculated by Wardle‡ |
| Bulk density (Mg $m^{-3}$) | 1.07 | 1.16 | S | 0.086 |
| Penetration resistance (0 to 20 cm) (MPa) | 2.76 | 3.04 | S | 0.217 |
| Penetration resistance (20 to 40 cm) (MPa) | 3.55 | 3.50 | NS | 0.836 |
| Carbon (%) | 4.67 | 4.25 | S | 0.259 |
| Respiration (μl $O_2$ $hour^{-1}$ $g^{-1}$) | 67.1 | 50.7 | S | 0.045 |
| Mineralizable N (mg $kg^{-1}$) | 140.3 | 106.2 | S | <0.001§ |
| Ratio of mineralizable N to C (mg $g^{-1}$) | 3.05 | 2.57 | S | 0.014 |
| Topsoil thickness (cm) | 22.6 | 20.0 | S | 0.013 |
| CEC (cmol $kg^{-1}$) | 21.6 | 19.7 | S | 0.306 |
| Total N (mg $kg^{-1}$) | 4717 | 4317 | S | 0.331 |
| Total P (mg $kg^{-1}$) | 1623 | 1639 | NS | 0.962 |
| Extractable P (mg $kg^{-1}$) | 50.2 | 63.6 | S | 0.341 |
| Extractable S (mg $kg^{-1}$) | 11.6 | 18.7 | S | 0.336 |
| Extractable Ca (cmol $kg^{-1}$) | 12.7 | 13.5 | NS | 0.599 |
| Extractable Mg (cmol $kg^{-1}$) | 1.77 | 1.50 | NS | 0.294 |
| Extractable K (cmol $kg^{-1}$) | 1.09 | 1.01 | NS | 0.704 |
| pH | 6.10 | 6.25 | S | 0.135 |

*Calculated from data in table 2 of (*1*). †Analysis of variance (ANOVA), $P < 0.01$, from table 3 of (*1*). ‡Value of *P* from two-way ANOVA. §Statistically significant at $P < 0.01$.